Proceedings of the Sixth International Conference on
Railway Technology: Research, Development and Maintenance
Edited by: J. Pombo
Civil-Comp Conferences, Volume 7, Paper 18.7
Civil-Comp Press, Edinburgh, United Kingdom, 2024
ISSN: 2753-3239, doi: 10.4203/ccc.7.18.7

Design of Geogrid Stabilisation for Railway Ballast and Subballast

F. Trovato[1] and P. Rimoldi[2]

[1]Geosynthetic Business Unit, Officine Maccaferri Spa
Bologna, Italia
[2]Milano, Italy

Abstract

Railways face unique challenges on soft soils due to heavy loads exerted on the subgrade by passing trains. This can lead to rapid and repetitive loading, causing settlements that compromise railway integrity. To address this, reinforcing geogrids can be used to stabilize the railway base, extending its lifespan. This paper presents a methodology for designing geogrid stabilization systems tailored to railway ballast and subballast. Factors such as wheel loads, traffic frequency, and subgrade properties are considered in the design process, which adapts established principles from road base stabilization. By integrating these principles, the methodology aims to provide a systematic approach for effectively incorporating geogrids into railway infrastructure projects, ultimately enhancing stability and longevity.

Keywords: geogrid, stabilization, railway design, ballast bed, subballast, cyclic loading.

1 Introduction

Railways, often established on soft terrain, pose unique challenges regarding the distribution of loads: a single train can generate hundreds of wheel loads within seconds, resulting in rapid, repetitive, and cyclical loading patterns. These loads are initially absorbed by the rails, then transferred through the sleepers, ballast, and potentially the subballast, consistently affecting the same area. The impact of these loads on soft soil leads to both absolute and differential settlements, swiftly compromising the integrity of the railway. The primary role of the railway

superstructure is to evenly distribute the axial loads of the wheels into the subgrade. However, if the railway superstructure fails to efficiently transmit these loads to the ballast, subballast, and ultimately to the subgrade, significant deformations may occur, necessitating speed reductions along the track. Incorporating layers of geogrid for stabilizing the ballast and/or subballast helps to mitigate settlements, ensuring structural durability and enhanced operational efficiency. While design methodologies for geogrid stabilization exist for road bases, reliable methods for stabilizing railway ballast and subballast are lacking.

This paper introduces a design approach for geogrid-stabilized railway ballast and subballast, considering factors such as wheel loads, frequency of wheel passes, railroad geometry, subgrade characteristics, and geogrid properties. Building upon established engineering principles, this method extends existing techniques for designing stabilized road bases. It incorporates the latest research findings on railway ballast behaviour and properties, ensuring a comprehensive and effective design approach.

2 Geometry and materials

The railway superstructure comprises the ballast, optional subballast, sleepers, and rails. Ballast, typically made of sharp-edged stones ranging from 20 to 100 mm, is placed above the subballast or directly on the subgrade to stabilize rails and sleepers. It distributes loads, absorbs temperature changes, and restricts lateral and vertical movements. Subballast, typically composed of granular material such as mix of sand and gravel, enhances load distribution and protects against fine particle and ice intrusion. National regulations specify a minimum ballast thickness of around 500 mm for main lines and 350 mm for secondary lines, with subballast typically 200-300 mm thick. In soft subgrade or poor geotechnical conditions, thickness may increase significantly for both ballast and subballast

Figure 1 depicts the layout of a single-track railway line in Italy, where the distance between the axes of the rails measures 1.435 m. Figure 2 illustrates the standard geometry of sleepers, with characteristic dimensions of length (L) x width (W) x height (H) at 2.60 m x 0.26 m x 0.16 m, respectively. Sleepers are typically positioned at intervals ranging from 0.60 m to 0.80 m. Regarding rail geometry, a Vignole type rail, as per EN 13674-1 standards [1], features a base width of 150 mm.

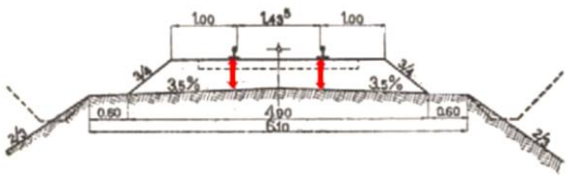

Figure 1: The railway superstructure

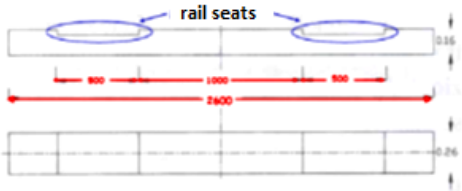

Figure 2: Cross section and plan view of a sleeper

3 Existing design methods for ballasted railway tracks

The design of ballasted railway track foundations relies on accurately estimating the thickness of granular layers (ballast and subballast) to withstand dynamic loads from passing trains, often using the North American Railway Method. The American Railway Engineering Association (AREA) [2][3], recommends a total granular layer thickness of 450 mm, with specific minimum thicknesses for ballast and sub-ballast of 300 mm and 150 mm respectively. According to AREA manual the main steps for railway track design steps involve determining the design rail seat load P_d and sleeper/ballast contact pressure σ_{sb}, ensuring the subgrade stress matches the allowable bearing pressure. Raymond [4] proposed considering subgrade strength based on Casagrande soil classification.

Existing methods, like British Railways [5] and Li and Selig[6][7], address the effects of repeated loading on plastic strain and deformation. However, they may overlook certain aspects, such as the impact of subgrade layer thickness or the deformation of the ballast layer [8][9].

4 Development of a new design method

Geogrid stabilization offers a practical solution for strengthening railway bases, including ballast and/or subballast, to mitigate settlements and increase the life cycle. A systematic design approach for geogrid-stabilized railway ballast/subballast has been developed, considering factors like wheel loads, frequency of passages, railway geometry, subgrade characteristics, and geogrid properties. This design method is built upon the principles established by the Leng and Gabr method [10][11][12] for designing geogrid stabilization in road bases, adhering to the same engineering fundamentals. Additionally, it represents an evolution of the method presented by Rimoldi [13].

4.1. Stabilisation of the ballast

Leng and Gabr introduced a method for designing geosynthetic-stabilized unpaved roads, which analyses the distribution of vertical stresses, the correlation between bearing capacity mobilization, rutting depth, and geogrid modulus at 2% strain. This method was validated through experimental tests. Adapting this method to railways, particularly for ballast stabilization without subballast, involves placing geogrids at the base of the ballast as shown in Figure 3. The method assumes a paved road section as a two-layer system with different elastic moduli.

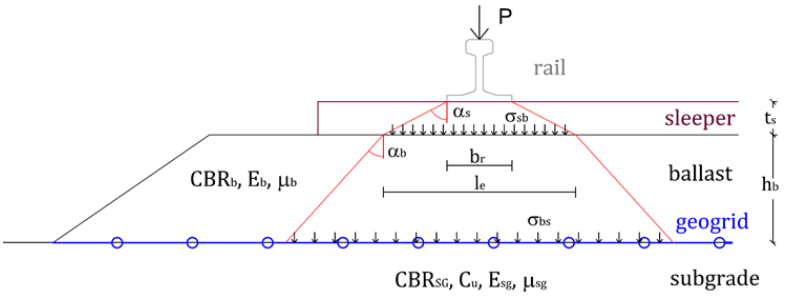

Figure 3: Schematic of the model for the stabilisation of ballast

Odemark's theory [14] transforms a multi-layered system into an equivalent system, where layer thickness adjusts to ensure that all layers have the same elastic modulus. This equivalent system behaves like an elastic half-space, allowing application of Boussinesq theory to determine stress distribution due to applied stress on the surface.

In the context of a two-layer system consisting of ballast and subgrade (Figure 4a), the equivalent thickness of the ballast (he), ensuring it matches the elastic modulus of the subgrade (E_{sg}), is given by:

$$h_e = h_b \cdot \left[\frac{E_b \cdot (1-\mu_{sg}^2)}{E_{sg} \cdot (1-\mu_b^2)}\right]^{1/3} = h_b \cdot \chi_1 \quad (1)$$

where: h_b = thickness of the ballast (m), E_b = elastic modulus of the ballast (kPa), E_{sg} = elastic modulus of subgrade (kPa), μ_b = Poisson's ratio of the ballast (default value = 0.35), μ_{sg} = Poisson's ratio of the subgrade (default value = 0.42); χ_1 = Odemark coefficient ballast – subgrade.

When there is also the subballast (Figure 4b), the thickness h_e, calculated for a single granular layer, has to be increased to the equivalent thickness h_g of the granular layers (ballast + subballast), given by:

$$h_g = h_e \cdot \left[\frac{E_b \cdot (1-\mu_{sb}^2)}{E_{sb} \cdot (1-\mu_b^2)}\right]^{1/3} = h_e \cdot \chi_2 \quad (2)$$

where: E_{sb} = elastic modulus of subballast, μ_{sb} = Poisson's ratio of the subballast (default value = 0.30); χ_2 = Odemark coefficient ballast – subballast.

a)

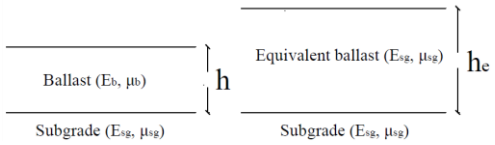

b)

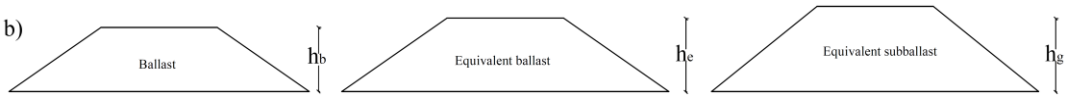

Figure 4 a) Transformation of the actual system in an equivalent one with a modulus equal to that of the subgrade; b) Case of ballast and subballast

The matter is: which modulus should be used? In railway design the initial modulus E_i, the resilient unloading – reloading modulus E_{ur}, and the secant modulus E_{50} are often used. Since there is no uniformity, in the presently proposed design method the following formulas, commonly used in road engineering, are used to calculate the modulus:

- Modulus of the subgrade E_{sg} (MPa) (Shell formula, from [15]), valid for fine soils with CBR ≤ 10:

$$E_{sg} = 10 \cdot CBR_{sg} \quad (3)$$

- Modulus of the ballast E_b (MPa) and subballast E_{sb} (MPa) (from [16]):

$$E_b = 36 \cdot CBR_b^{0.3} \qquad E_{sb} = 36 \cdot CBR_{sb}^{0.3} \quad (5)$$

with: CBR_{sg} = CBR index of the subgrade, CBR_b = CBR index of the ballast.

It must be noted that experimental evidence indicates that the modulus of limestone ballast is usually lower than the modulus of basalt and granite ballast; hence it is suggested to assume $CBR_b = 90$ for limestone ballast, and $CBR_b = 100$ for basalt and granite ballast. For suballast typical values are: $CBR_{sb} = 20 \div 30$.

With the Odemark transformation espressed by equation (1), the half space below the sleeper become uniform, elastic and isothropic, that is in the conditions for the validity of the well known Boussinesq theory.

The present method assumes that the vertical stresses are distributed through the equivalent granular layer according to Boussinesq theory for rectangular loaded area [17]. If the load from sleeper to ballast is assimilated to a uniform load on a rectangular area, the Boussinesq theory allows to obtain the value of the vertical stress σ_c at any point along the vertical line passing by one corner of the rectangle. With reference to Boussinesq theory and applying the following equations (8) and (9)

$$R_1 = (L^2 + z^2)^{0.5} \quad R_2 = (B^2 + z^2)^{0.5} \quad R_3 = (L^2 + B^2 + z^2)^{0.5} \tag{8}$$

$$\sigma_z = \frac{q}{2\pi} \cdot \left[\arctan\left(\frac{L \cdot B}{z \cdot R_3}\right) + \frac{L \cdot B \cdot z}{R_3} \cdot \left(\frac{1}{R_1^2} + \frac{1}{R_2^2}\right)\right] \tag{9}$$

it is possible to calculate the ratio of the vertical stress at top and bottom of ballast as:

$$\frac{\sigma_{sb}}{\sigma_{bs}} = \frac{\pi}{2} \cdot \frac{1}{\left[\arctan\left(\frac{L \cdot B}{z \cdot R_3}\right) + \frac{L \cdot B \cdot z}{R_3} \cdot \left(\frac{1}{R_1^2} + \frac{1}{R_2^2}\right)\right]} \tag{10}$$

where: σ_z = induced vertical stress at depth z below one corner of the rectangle (kPa), q = uniform pressure on the rectangular area (kPa); z = depth below surface (m); L, B = length and width of the rectangle (m).

4.2. Load Transfer

In a ballasted railway track, the rails transfer the wheel loads to the supporting sleepers, which are spaced evenly along the rail length. Similarly, sleepers transfer the load from the rail to the wider ballast area. The ballast and subballast layers transmit the high imposed stress at the sleeper/ballast interface to the subgrade layer at a reduced level through spreading.

In the presently proposed method, instead, the load from the rail spreads inside the sleeper according to the load spreading angle αs, that is symmetrically to the rail center (Figure 3). For standard concrete sleepers the value αs = 55° provides a value le practically equivalent to the value provided by the AREA method, while the value αs = 60° provides a value le practically equivalent to the value provided by the JNR method [18].

The load spreading angle should be assumed as: αs = 55° ÷ 60°. The effective length of sleeper le becomes:

$$l_e = b_r + 2 \cdot t_s \cdot \tan \alpha_s \tag{11}$$

where: l_e = effective length of sleeper (m); b_r = rail width (m); t_s = sleeper thickness (m). The sleeper/ballast contact area A_{sb} (m^2) and contact pressure σ_{sb} (kPa) are therefore:

$$A_{sb} = l_e \cdot b_s \quad (12)$$

$$\sigma_{sb} = P / (l_e \cdot b_s) \quad (13)$$

where: P = design rail seat load (kN); b_s = sleeper width (m).

In equation (13) for calculating the average sleeper/ballast contact stress, note that the rail seat load (P) differs from the wheel load (Pd = W / 2). The USACE manual [19] suggests distributing the point wheel load to five adjacent sleepers, emphasizing the load on the sleeper below the wheel. However, track deflection shows that only three sleepers bear the load, while others remain suspended. Additionally, research indicates that 40% to 60% of the wheel load is supported by the sleeper directly beneath the wheel.

Based upon the rail effectively distributes the load of 3 to 5 sleepers. In the more conservative scenario, where the load is shared by 3 sleepers, 50% of the load directly stresses the sleeper beneath the axle of the train, while each of the two adjacent sleepers bears 25% of the load from the axle. Consequently, if we denote W as the axle load, the rail seat load P generated by a wheel on the most heavily loaded sleeper can be approximated as:

$$P = 50\ \% \cdot W / 2 = W / 4 \quad (14)$$

With regard to the loads generated by the wheels of trains, the Eurocode load model LM71 for railway bridge loading from EN 1991-2 (2003) [20] can be considered, which is composed of 4 x 250 kN axles arranged with spacing of 1.60 m. In case of high-speed trains, the heaviest axle load (in driving cars) is typically equal to 170 kN/m. Hence, for train load like LM71: P = 250 / 4 = 62.5 kN. For a high speed train, the highest rail seat load can be assumed as: P = 170 / 4 = 42.5 kN.

4.3. Design rail seat load

To consider the dynamic component of wheel load, the static wheel load shall be multiplied by an influence coefficient generally known as the dynamic amplification factor (DAF). Many factors affect the DAF, including train speed, static wheel load and wheel diameter, unsprung vehicle mass, condition of vehicle and track-ground system, etc. In the existing design methods, a variety of empirical equations can be used for determining the design vertical wheel load. In these methods, the design dynamic wheel load is generally expressed as a function of the static wheel load.

In the presently proposed method, according to [6][7], the AREA impact factor will be used:

$$P_{dyn} = \varphi \cdot P \quad (15)$$

where: P_{dyn} and P are the dynamic and static wheel load (kN), respectively; and φ is the dimensionless DAF, which is given by:

$$\varphi = 1 + \frac{0.0052\ C}{D_w} \quad (16)$$

where: C is the train speed (km/h), and D_w is the wheel diameter (m).

For cargo trains the following typical values can be assumed: C = 100 km/h, and D_w= 0.90 m; hence a typical value of DAF is: φ = 1.58.

For high speed trains the following typical values can be assumed: C = 300 km/h, and D_w = 0.92 m; hence a typical value of DAF is: φ = 2.70. The design rail seat load should be assumed equal to:

$$P_{dyn} = \varphi \cdot W / 4 \quad (17)$$

4.4. Applied Stress on Subgrade

The load spreading model here assumed is the trapezoidal distribution, as proposed by Indraratna et al. [21], shown in Figure *5*. The trapezoidal approximation is a simple approach for estimating the variation in vertical stress with depth. According to this method, it is assumed that the vertical stress diminishes with depth in the form of a trapezoid according to the load spreading angle, α_b, as shown in Figure *5Figure 1*.

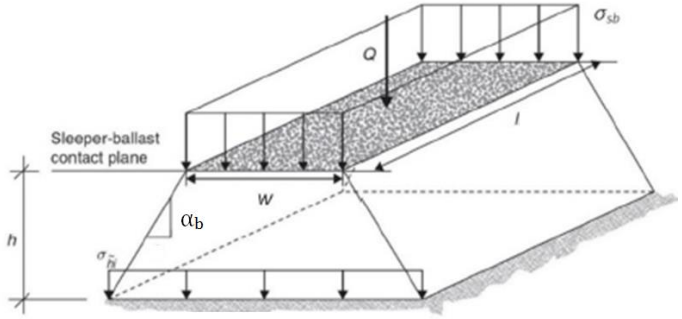

Figure 5: Stress distribution on the subgrade from sleeper/ballast contact stress by trapezoidal distribution (modified from [21])

Subsequently, the stress at the equivalent depth he below the sleeper is:

$$\sigma_{bs} = \sigma_{sb} \cdot \frac{A_{bs}}{A_{sb}} \quad (18)$$

$$A_{sb} = l_e \cdot b_s \quad (19)$$

$$A_{bs} = (l_e + 2 \cdot h_e \cdot \tan\alpha_b) \cdot (b_s + 2 \cdot h_e \cdot \tan\alpha_b) \quad (20)$$

where: σ_{sb} is the average value of vertical stress below the sleeper (i.e. above the ballast), from Equation (13); A_{sb} is the sleeper/ballast contact area; A_{bs} is the ballast / subgrade contact area; and h_e is the equivalent thickness of ballast, from equation (1).

4.5. Allowable settlement

The allowable settlement of the rail tracks is very limited, of the order of 1 to 5 mm; above these values trains are bound to reduced speed. At the base of the ballast or sub-ballast allowable settlements are larger, since only part of the settlements at subgrade interface is transmitted to the sleepers and rails. According to [22], the thresholds for permanent allowable settlements of rails must be considered in accordance with the requirements of railway feasibility, which are of the order of a few millimeters. Such low values can be considered in the presence of a light seismic event, while for heavy seismic events a threshold of tolerance shall be of the order of several centimeters, which has a sense not so much as to ensure the practicability but as to allow a rapid recovery. Therefore, it can be assumed that the settlement limit at the interface with the subgrade is equal to 50 mm, while the settlement limit at the top of ballast can be assumed equal to 5 mm.

4.6. Accumulated plastic deformation of ballast

For unstabilised ballast, Sayeed has proposed an improved empirical model, which is a modification of a model previously suggested by Shahin [23], for better prediction of the accumulated plastic deformation of ballast.

In the present method, a modification of the Sayeed [24] model is used for the evaluation of the accumulated plastic deformation of unstabilised ballast; the modified model is expressed by the following formula:

$$\varepsilon_{bu} = x \cdot \alpha^{y} \cdot [1 + \ln (N)]^{\nu} \quad (21)$$

where ε_{bu} is the cumulative plastic strain of unstabilised ballast (%); N is the number of load applications on the ballast; and α, x, y and ν are regression parameters depending on the ballast type as summarized in Table 1 (modified from [7]).

At present there are no published method for evaluating the accumulated plastic deformation of stabilised ballast. As reported by Rimoldi, Vecchiotti and di Prisco [25] have studied the behavior of railway superstructures by: theoretical analysis of the problem; experimental tests on a small scale; formulation of a numerical model to interpret the experimental results and predict real-scale settlements; development of a method for the estimation of settlements. The model of Vecchiotti and di Prisco allowed to interpret the experimental data and to set the following formula for the estimation of the settlement r:

$$r = \beta \, \text{Log} \, N \quad (22)$$

with: N = number of load cycles; β = coefficient depending on the applied load.
The formulas for calculating the coefficient β are:

- for unstabilised ballast: $\beta_u = (0.0655 \, P_{dyn} - 0.8256)$ (23)
- for stabilised ballast: $\beta_s = (0.05163 \, P_{dyn} - 0.4245)$ (24)

with: P_{dyn} = design rail seat load (kN), from Equation (15).

Hence, in absence of any other data, in the present method the accumulated plastic deformation of stabilised ballast ε_{bs} is evaluated as:

$$\varepsilon_{bs} = \varepsilon_{bu} \cdot (\beta_s / \beta_u) \quad (25)$$

Table 1. Material parameters for various types of ballast (modified from [8])

Ballast type	x	y	ν	α
Basalt	4.82	1.42	0.49	0.30
Granite	1.27	2.41	0.48	0.67
Dolomite	4.23	1.15	0.32	0.40

4.7. Prediction of subgrade deformation

As reported by Sayeed, based on experimental data collected from tests, various models were proposed for estimating the cumulative plastic strain of fine-grained soils under repeated loading. Among these models, the most advanced ones that are currently used to predict the cumulative plastic strain and cumulative plastic

deformation of track fine-grained subgrade soils are the ones presented by Li [26] and Li and Selig [27], which are modified in the present method as following:

$$\varepsilon_{sp} = \frac{\xi}{100} \cdot N^{\vartheta} \cdot \left(\frac{\sigma_{bs}}{q_c}\right)^{\omega} \quad (26)$$

$$r_u = \varepsilon_{sp} \cdot H_s \quad (27)$$

$$r_u = \sum_{i=1}^{n} \varepsilon_{spi} \cdot H_{si} \quad (27\ bis)$$

where: ε_{sp} is the cumulative plastic strain of track subgrade soil; σ_{bs} is the vertical stress applied at the ballast – subgrade interface; q_c is the bearing capacity of the subgrade soil; N is the number of load repetitions in the subgrade; ξ, ϑ and ω are material parameters given in Table 2; r_u is the rut depth at the ballast – subgrade interface in case of unstabilised ballast / subballast; H_s is the thickness of the soft subgrade layer; ε_{spi} and H_{si} are the cumulative plastic strain and layer thickness for the i-th subsoil layer, in case of stratified subsoil. For practical calculations, as required for design purposes, the considered thickness of the soft subgrade may be limited to 5.0 m. At present there are no published method for evaluating the rut depth at the ballast-subgrade interface in case of stabilised ballast / subballast.

Due to lack of any other data, as done above, in the present method the rut depth at the ballast – subgrade interface in case of stabilized ballast/subballast is evaluated as:

$$r_s = r_u \cdot (\beta_s / \beta_u) \quad (28)$$

Table 2. Material parameters for various types of soil (modified from [26] and [27]).

Subgrade soil type	ξ	ω	ϑ
Fat clay (CH)	1.20	2.4	0.18
Lean clay (CL)	1.10	1.8	0.16
Elastic silt (MH)	0.84	2.0	0.13
Silt (ML)	0.64	1.7	0.10

4.8. Calculation of the load spreading angle in ballast

We have previously assumed the trapezoidal distribution of the load inside the ballast; now, for simplifying calculations, let's reduce the rectangular loaded area below the sleeper to a square load area of size a_t, having the same area of the rectangular one; hence:

$$a_t = (l_e \cdot b_s)^{0.5} \quad (29)$$

With reference to Figure 5, still considering the trapezoidal distribution according to the load spreading angle α_b, the square loaded area at the ballast – subgrade interface will have size $a_b = a_t \cdot \tan \alpha_b$.

The load from sleeper to ballast shall be the same load that is transferred to the subgrade; hence, considering the equivalent thickness h_e (see Equation (1) and Figure 4.a), it shall be:

$$\sigma_{sb} \cdot a_t^2 = \sigma_{bs} \cdot a_b^2 = \sigma_{bs} \cdot (a_t + 2 \cdot h_e \cdot \tan\alpha_b)^2 \quad (30)$$

Therefore, we can calculate the load spreading angle α_b, to be intended as the value at the first application of the train wheel load α_{b1}, as:

$$\tan\alpha_{b1} = \frac{a_t}{h_e} \cdot \left(\sqrt{\frac{\sigma_{sb}}{\sigma_{bs}} - 1} \right) \quad (31)$$

where (σ_{sb} / σ_{bs}) has to be calculated with equation (10).

4.9. Degradation of the load spreading angle with loading cycles

Based on cyclic plate load tests[10], it has been shown that the spreading angle α_b of the load decreases with the number of load cycles. This corresponds to the intuitive concept that a large number of wheel passages results in a degradation of the ballast, due to the displacement of the grains of soil and the horizontal tensile stresses that are generated because of Poisson's ratio of the ballast, which in turn causes a decrease in the elastic modulus E_b of the ballast: since a less rigid layer spreads the loads worse than a hard layer, it is intuitive that as the number of passages increases the load spreading angle decreases. Therefore Leng and Gabr [10] introduced the coefficient λ_2 of degradation of the angle α, defined as:

$$\lambda_2 = \frac{\tan\alpha_{bN}}{\tan\alpha_{b1}} = \frac{1}{1+k_2 \cdot \log N} \quad (32)$$

where: tan α_{bN} = tangent of the angle of load distribution at the N-th loading cycle, tan α_{b1} = tangent of the initial angle of load distribution (for N = 1) from Equation (31); N = number of load cycles, k_2 = parameter that defines the degradation of tanα_b.

4.10. Effect of geogrids for stabilisation of ballast

Based on cyclic plate load tests [10] and in situ tests [28], it was shown that the introduction of geogrid stabilisation in the ballast delays and minimizes the degradation of the load spreading angle with the number of passages. In fact, the open structure of geogrids allows the interlocking of the grains of soil, so that the grains are confined by the geogrid, which provides tensile forces at low strain; interlocking and geogrid tensile forces (which produce horizontal compressive stresses on soil granules) prevent lateral movement and expansion of soil under load, produced by the Poisson's ratio of the soil. Thus, the elastic modulus of the ballast is maintained for much longer as the number of passages increases and consequently the degradation of the angle of load diffusion decreases. Based on the above experimental evidence and empirical criteria, the influence of the geogrid is introduced by Leng and Gabr by means of the tensile strength of geogrids $T_{2\%}$ at 2% strain. The coefficient k_2, which defines the degradation of α_b, is related to the tensile strength of geogrids $T_{2\%}$ by the following empirical equation:

$$k_2 = (a_t / h)^{0.81} \cdot \text{Max}\left[(0.58 - 0.000046\, T_{2\%}^{4.5}), 0.15\right] \quad (33)$$

The minimum value of k_2 is for N = 1 and is equal to 0.15. Equation (33) contains the intuitive fact that as the thickness h of the ballast increases the degradation of α_b (and then the coefficient k_2) is decreased.

4.11. Bearing capacity mobilization factor

The load bearing capacity of the subgrade, according to the scheme in Figure 3, is defined with the classic formula:

$$q_c = N_c \cdot c_u \quad (34)$$

where: N_c = bearing capacity factor; c_u = undrained shear strength of subgrade (kPa).

Leng and Gabr [10] assumed the following values for the bearing capacity factor N_c:

- N_c = 3.80 for unstabilised unpaved roads (N_c value in the case of saturated cohesive soil conditions at the elastic limit in axially symmetric conditions);
- N_c = 6.04 for unpaved roads stabilised with geogrids (N_c value in the case of saturated cohesive soil with maximum shear stress at the interface).

The same N_c values will be assumed here for unstabilised and stabilised railway ballast and subballast.

The well known empirical relation between CBR_{sg} value and the undrained shear strength of subgrade c_u (kPa) can be used (Giroud and Han [16]):

$$c_u = 30 \cdot CBR_{sg} \tag{35}$$

Leng and Gabr introduced the bearing capacity mobilization factor, m, which allows the expression of mobilized resistance as a function of the bearing capacity and the vertical stress applied on subgrade:

$$m = N_{cm} / N_c = \sigma_{bs} / (N_c \cdot c_u) \tag{36}$$

where: N_c = bearing capacity factor of the subgrade; N_{cm} = mobilized bearing capacity factor of the subgrade; c_u = undrained cohesion of the subgrade.

Leng and Gabr, based on experimental evidence, found the following empirical relationship:

$$m = \left(1 - e^{-0.78 \cdot \left(a_t / h\right)}\right) \cdot \frac{N_{cm}}{N_c} \tag{37}$$

The mobilization of bearing capacity of the subgrade occurs at the cost of a settlement on the upper surface of the subgrade itself, i.e. in proportion to the depth of the rut that is created at the ballast – subgrade interface. Leng and Gabr [12] assumed that at the critical value r_{cr} of the rut depth the entire load-bearing capacity of the subgrade is mobilised; the critical rut r_{cr} (m) is related to the number of passes through the following empirical relationship:

$$r_{cr} = 0.025 \cdot (0.125 \cdot \log N + 1.5) \tag{38}$$

By assuming that the mobilization of bearing capacity increases linearly with the depth of rutting r at the ballast – subgrade interface, Equation (37) becomes:

$$m = \left[1 - e^{-0.78 \cdot \left(a_t / h\right)}\right] \cdot \frac{r}{r_{cr}} \tag{39}$$

where the rut depth r has to be calculated with Equation (27) for unstabilised ballast, and with Equation (28) for stabilised ballast.

The mobilized bearing capacity q_{cm} becomes:

$$q_{cm} = m \cdot N_c \cdot c_u \tag{40}$$

4.12. Minimum thickness of ballast

The vertical stress at ballast – subgrade interface σ_{bs} shall be less than the load bearing capacity mobilized in the subgrade, so as not to cause failure of the subgrade due to an excess of localized settlements, that is of rut depth. Still considering the load from

sleeper to ballast applied on a square area of size a_t, and the trapezoidal distribution of load in ballast (Figure *5*), the following condition shall be verified:

$$\sigma_{bs} = \frac{P_{dyn}}{(a_t + 2 \cdot h \cdot \tan\alpha_{bN})^2} \leq m \cdot N_c \cdot c_u \tag{41}$$

From equation (41) we obtain the minimum thickness h of ballast:

$$h = \frac{1}{2 \cdot \tan\alpha_{bN}} \cdot \left(\sqrt{\frac{P_{dyn}}{m \cdot N_c \cdot c_u}} - a_t \right) \tag{42}$$

The model described above is based on the results of cyclic loading tests performed in the laboratory (Leng and Gabr). To make the method more closely to actual conditions, a model factor, equal to 0.85, is introduced in Equation (42); then, assuming that the degradation of the load spreading angle in ballast with the number of passes is given by Equation (32), Equation (42) becomes:

$$h = \frac{0.85 \cdot (1 + k_2 \cdot \log N)}{2 \cdot \tan\alpha_{b1}} \cdot \left(\sqrt{\frac{P_{dyn}}{m \cdot N_c \cdot c_u}} - a_t \right) \tag{43}$$

Since (P_{dyn} / a_t^2) shall be equal to the vertical stress transmitted from sleeper to ballast, σ_{sb}, Equation (43) can be rewritten as:

$$h = \frac{0.85 \cdot a_t \cdot (1 + k_2 \cdot \log N)}{2 \cdot \tan\alpha_{b1}} \cdot \left(\sqrt{\frac{\sigma_{sb}}{m \cdot N_c \cdot c_u}} - 1 \right) \tag{44}$$

Considering that the thickness h of the base appears in both members of Equation (43) or Equation (44), they should be solved by an iterative process.

By solving Equation (43) with respect to the load P_{dyn}, we obtain the following equation:

$$P_{dyn} = m \cdot N_c \cdot c_u \cdot \left(\frac{2 \cdot h \cdot \tan\alpha_{b1}}{0.85 \cdot (1 + k_2 \cdot \log N)} + a_t \right)^2 \tag{45}$$

By solving Equation (44) with respect to the vertical stress σ_{sb} we obtain the following equation:

$$\sigma_{sb} = m \cdot N_c \cdot c_u \cdot \left(\frac{2 \cdot h \cdot \tan\alpha_{b1}}{0.85 \cdot a_t \cdot (1 + k_2 \cdot \log N)} + 1 \right)^2 \tag{46}$$

Equation (45) or Equation (46) can be used to calculate h when the P_{dyn} or σ_{sb} value is known: starting with a minimum value of h (e.g. h = 0.15 m), h is increased in small steps until the value calculated with Equation (45) or Equation (46) becomes equal to the known value P_{dyn} or σ_{sb}.

Equations (43), (44), (45), and (46) afford to calculate the minimum thickness both for unstabilised ballast, h_u, and for stabilised ballast, h_s: for unstabilised ballast, the parameter k_2 has to be calculated from Equation (33) with $T_{2\%} = 0$, and the parameter m has to be calculated using the rut depth ru from Equation (27); for stabilised ballast the coefficient k_2 has to be calculated from Equation (33) with the $T_{2\%}$ value for the selected geogrid, and the parameter m has to be calculated using the rut depth rs from

Equation (28). The value of h used at each iteration influences the parameters k_2, tan α_{b1}, and m.

4.13. Stabilisation of the subballast

When the total granular thickness h'_g is composed of the ballast thickness h'_b and subballast thickness h'_{sb} (Figure 4b), from Eqs. (1) and (2) we get:

$$h'_g = h_e \cdot \chi_2 \tag{47}$$

$$h'_b = \frac{h_g}{\chi_1 \cdot \chi_2} \tag{48}$$

$$h'_{sb} = h_g - h'_b \tag{49}$$

The above formulas can be used to calculate the thickness of ballast and subballast both in the unstabilised and stabilised cases.

If a set stabilized ballast thickness than h'_b is desired, it is possible to set the stabilized ballast thickness h''_{bs}.

In this case the stabilized subballast thickness has to be recalculated, which can be done by considering the increase or decrease in equivalent ballast thickness:

$$\Delta h_{bs} = (h'_{bs} - h''_{bs}) \cdot \chi_1 \tag{50}$$

The granular thickness becomes:

$$h''_g = h'_g + \Delta h_{bs} \tag{51}$$

The stabilized subballast thickness, with the set h''_{bs} stabilized ballast thickness, becomes:

$$h''_{sbs} = h''_g - h''_{bs} \tag{52}$$

Note that, for the stabilised design with ballast and subballast, the above formulas are valid only if both ballast and subballast are stabilised with geogrids having the same tensile strength at 2 % strain, $T_{2\%}$; anyway the opening size of the geogrid for ballast stabilisation and for subballast stabilisation need to be different and suited to the granular size distribution of the two materials.

Compared to the case of design with ballast only, the design with ballast and subballast requires a higher total granular thickness, yet the thickness of ballast gets reduced.

5 Conclusions

The paper presents a design method for geogrid stabilised railway ballast and subballast, which considers the wheel loads, the number of wheel passes, the geometry of the railroad, the characteristics of the subgrade and the properties of geogrids.

The proposed design method is an extension of Leng and Gabr method [10][11][12] for the design of geogrid stabilisation of road bases, and it is based on the same engineering principles.

For the development of the design method the latest research on the behavior of unstabilised ballast, subballast, and subgrade under railway loading has been considered.

The authors believe that the proposed design method for geogrid stabilised ballast and subballast is an important advancement, which will allow important savings in the use of selected granular materials in railway projects.

References

[1] EN 13674-1:2011+A1:2017 "Railway applications - Track - Rail - Part 1: Vignole railway rails 46 kg/m and above." *CEN*, Bruxelles, Belgium.

[2] AREA 1996 Manual for Railway Engineering **1** *American Railway Engineering Association (AREA)*, Washington, DC, USA

[3] AREMA 2003 Practical Guide to Railway Engineering, American Railway Engineering and Maintenance of Way Association. *Simmons-Boardman Publishing Corporation*. Maryland, USA

[4] Raymond G P 1978 "Design for railroad ballast and subgrade support." *Journal of the Geotechnical Engineering Division* **104** pp 45-60

[5] Heath D L, Shenton M J, Sparrow RW, and Waters JM 1972 Design of conventional rail track foundations. *Proceedings of the Institution of Civil Engineers* **51** pp 251-67

[6] Li D and Selig E T 1998a Method for railroad track foundation design. I: Development. *Journal of Geotechnical and Geoenvironmental Engineering* **124** p 316

[7] Li D and Selig E T 1998b Method for railroad track foundation design. II: Applications. *Journal of Geotechnical and Geoenvironmental Engineering* **124** p 323

[8] Li D, Hyslip J, Sussmann T, and Chrismer S 2002 *Railway Geotechnics*. CRC Press, Tailor & Francis Group, Broken Sound Parkway, NW, USA

[9] Stewart H E 1982 The prediction of track performance under dynamic traffic loading. *PhD Thesis, University of Massachusetts*, Amherst, Massachusetts, USA

[10] Leng J and Gabr M A 2002 Characteristics of geogrid-stabilised aggregate under cyclic load. *Journal of Transportation Research Board*, No. 1786, National Research Council, Washington, DC, USA, pp 29-35, November 2002

[11] Gabr M A 2005 Numerical analysis of stress-deformation response in stabilised unpaved road sections *Geosynthetics International* **12** pp 111-9

[12] Leng J and Gabr M A 2006 Deformation-Resistance Model for Geogrid-Stabilised Unpaved Road. *Journal of Transportation Research Board*, No. 1975, National Research Council, Washington, DC, USA pp 146-54, November 2006

[13] Rimoldi P 2012 Design method for railway bases reinforced with geogrid. *Proc. 2nd International Conference on Transportation Geotechnics*. Sapporo, Japan.

[14] Odemark N 1949 Investigations as to the Elastic Properties of Soils and Design of Pavements According to the Theory of Elasticity. Statens Vag Institute Meddeland 77 Stockholm, Sweden.

[15] Heukelom W and Foster C R 1960 Dynamic testing of pavements. *Journal of Soil Mechanics and Foundations Division*. American Society of Civil Engineers **86** No. SM1.

[16] Giroud J P and Han J 2004 Design method for geogrid-stabilised unpaved roads – Part I: theoretical development. *ASCE Journal of Geotechnical and Geoenvironmental Engineering* **130**pp 776-86

[17] Facciorusso J, Madiai C, Vannucchi G 2011 Pressioni di contatto e diffusione delle tensioni in un semispazio elastic. *Dispense di Geotecnica*. University of Firenze, Italy (In Italian)

[18] Atalar C, Das B M, Shin E C, and Kim D H 2001 Settlement of geogrid reinforced railroad bed due to cyclic load. *Proceedings of the International Conference on Soil Mechanics and Geotechnical Engineering*, Istanbul pp 2045-8
[19] USACE 2008 Engineering Guidance Design Manual. 7th edition. *U.S. Army Engineering Support Center*. Huntsville, AL, USA
[20] EN 1991-2 2003 Eurocode 1: Actions on structures - Part 2: Traffic loads on bridges. *CEN*, Bruxelles, Belgium
[21] Indraratna B, Salim M W, and Rujikiatkamjorn C 2011a *Advanced Rail Geotechnology - Ballasted Track*. Taylor & Francis Group, London, UK
[22] Pagano L and Sica S 2009 Vulnerabilità delle reti viarie. In "*Costruzioni in terra*", Gruppo Nazionale per la Difesa dai Terremoti, Progetto VIA. Roma, Italy. (in Italian)
[23] Shahin M A 2009 Design of ballasted railway track foundations under cyclic loading. *Proceedings of the 2009 GeoHunan International Conference – Slope Stability, Retaining Walls, and Foundations*, Changsha, Hunan, China pp 68-73
[24] Sayeed A 2016 Design of Ballasted Railway Track Foundations using Numerical Modelling with Special Reference to High Speed Trains. *PhD thesis, Curtin University*. Perth, Australia
[25] Vecchiotti M and di Prisco C 2006 Comportamento Meccanico di Rilevati Ferroviari rinforzati sottoposti a carichi ciclici. *Proc. XVIII Convegno Nazionale Geosintetici. L'Ingegnere e l'Architetto*, n.1 (in Italian)
[26] Li D 1994 Railway track granular layer thickness design based on subgrade performance under repeated loading. *PhD Thesis, University of Massachusetts*, Amherst, Massachusetts, USA
[27] Li D and Selig E T 1996 Cumulative plastic deformation for fine-grained subgrade soils. *Journal of Geotechnical Engineering*, **122**pp 1006-13
[28] Fannin R J and Sigurdsson O 1996 Field Observations on Stabilization of Unpaved Roads with Geosynthetics. *ASCE Journal of Geotechnical Engineering*, **122** pp 544-53.